Nanostructured Catalysts for Sustainable Energy

Ariana Jensen, Liam McCormick
University of New York, Brooklyn, USA

***Abstract*—**Oxygen Reduction Reaction (ORR) performance of iron and nitrogen co-doped porous carbon nanoparticles (Fe-NPC) with various physical and (electro) chemical properties have been investigated. Fe-NPC nanoparticles are synthesized via a facile soft-templating procedure by using Iron (III) chloride hexa-hydrate as iron precursor and aminophenol-formaldehyde resin as both carbon and nitrogen precursor. Fe-NPC nanoparticles shows high surface area (443.83 m^2g^{-1}), high pore volume (0.52 m^3g^{-1}), narrow mesopore size distribution (ca. 3.8 nm), high conductivity (I_G/I_D=1.04), high kinetic limiting current (11.71 $mAcm^{-2}$) and more positive onset potential (-0.106 V) compared to metal-free NPC nanoparticles (-0.295V) which make it high efficient ORR metal-free catalysts in alkaline solution. This study may pave the way of feasibly designing iron and nitrogen containing carbon materials (Fe-N-C) for highly efficient oxygen reduction electro-catalysis.

***Keywords*—**Electro-catalyst, mesopore structure, oxygen reduction reaction, soft-template.

I. Introduction

NOWADAYS, energy is one of the most important challenges facing mankind due to its supply and demand issues as well as global warming [1], [2]. Among different solutions for the energy challenges, electrochemistry that deals with the conversion between electricity and energy stored in chemical bonds can be used to solve these realistic issues.[3], [4] Electrochemical energy conversion is based on electrochemical reactions at the surface of a certain electrode, which is a direct and clean process without any major impact to the environment. [4] Moreover, electrochemical energy systems can be applied as efficient and stable platforms for energy storage and conversion [5].

Oxygen Reduction Reaction (ORR) is one of the most important processes in energy conversion devices such as fuel cells [6], metal-air batteries [7] and chlor-alkali electrolysis [8]. However, the sluggish kinetics of ORR in nature significantly decreases the energy conversion efficiency, which therefore underline the importance of suitable electro-catalysts to promote ORR by reducing the reaction barrier and facilitating the reaction kinetics to achieve an efficient four electron (4e-) reaction.[9] Platinum based materials are the most widely used catalysts to improve the kinetics of ORR in fuel cells. Although they are effective due to their low over potential and excellent 4e- selectivity, but weak durability, limited stability, low active surface area, high cost and supply constraints do not allow their large-scale application [10], [11]. On the other hand, carbon-based materials show great potential compared to Pt-based catalysts featuring low-cost, high stability, excellent activity especially in alkaline medium and high durability against fuel methanol and carbon monoxide as an efficient 4e– ORR electro-catalysts owing to their unique electronic structures [12], [13]. Among the carbon-based electro-catalysts, carbon nanoparticles with porous structures and controlled morphologies have great advantages because of their remarkable properties including high surface area and the diffusion channels for fast mass transfer [14]. However, electro-catalysts are required to encompass good electrical conductivity for electron transfer and chemical stability besides high surface area and controlled nanostructure. Thus, heteroatoms and/or different metal species are usually doped into the chemical structure of carbon matrix to improve the overall conductivity of catalysts, provide more active sites, and enhance the interaction between carbon and other molecules by tuning electron donor/acceptor property of doped materials [15], [16]. We therefore anticipate that Fe-N-C structure with high surface area and pore volume could be a good candidate for ORR catalysis.

In this work, Fe, N co-doped porous carbon nanoparticles (Fe-NPC) are developed via a facile and low-cost soft-templating procedure using aminophenol-formaldehyde resin as carbon and nitrogen precursors and Iron (III) chloride hexa-hydrate as iron precursor. This catalyst has successfully combined the aptitudes including hierarchical porosity for facile reactant transportation and sufficient active site exposure as well as abundant graphitic carbon structure to maximize the conductivity and highly active Fe-N species, which has thus resulted in an excellent catalytic activity similar to commercial Pt/C for ORR.

II. Material and Methods

A. Chemicals

Plurinic (F127), Hexadecyltrimethylammonium bromide (CTAB, ≥98%), 3-Aminophenol (C_6H_7NO, 98%) and Iron (III) chloride hexahydrate ($FeCl_3.6H_2O$) were purchased from Sigma-Aldrich. Formaldehyde solution (HCHO, 37/10) and ethanol (EtOH, absolute) were purchased from Chem-Supply. Highly purified water (DI water, >18 MΩ cm resistivity) was provided by a PALL PURELAB Plus system. All chemicals were directly used without any further treatment and purification.

B. Material Synthesis

In a typical synthesis, 0.25 g of fully dissolved F127 in 20 ml of EtoH was added to 50 ml of DI-water at 25°C. Then 0.325 g Hexadecyltrimethylammonium bromide was added to the solution and kept stirred for 30 minutes. Next, 0.5 g 3-Aminophenol was added and stirred until a complete dissolution followed by introduction of 0.7 mL (37 wt. %) formaldehyde and stirred for another 30 minutes. Afterwards, a given amount of $FeCl_3.6H_2O$ (5 wt. %) was added to the mixture and kept stirring at 25°C for 24 hours. Finally, the mixture was transferred to a Teflon-lined

autoclave for hydrothermal reaction at 100 °C for 24 h. The resulting solid polymers were collected by vacuum filtration followed by washing with DI-water and ethanol for 3 times and drying at 100°C for 24 hours. This washing step leads to remove the free iron species, which were accessible outside of carbon framework. Fe-NPC nanoparticles were obtained by calcination of solid polymers under N_2 flow in the tubular furnace at 350°C using heating rate of (1°C/min) for 3 hours to remove the template followed by carbonization at 900°C with heating rate of (2°C/min) for 4 hours under N_2 flow. Iron-free catalysts (NPC) were synthesized for comparison purposes using the same synthesizing procedure.

C. Material Characterization

The morphology of synthesized samples was characterized by scanning electron microscope (FEI Quanta 450 ESEM) with EDS probe operating at 10 kV. Nitrogen adsorption-desorption isotherms were measured on Tristar II (Micrometrics) at -196°C. Pore size distributions were calculated by Barrett-Joyner-Halenda (BJH) model using the data of adsorption branch on the isotherm. The specific surface areas were calculated using adsorption data at the relative pressure range of P/P_0 = 0.05-0.3 by Brunauer-Emmett-Teller (BET) model. The total pore volumes were estimated from the adsorbed amounts at a relative pressure (P/P_0) of 0.994. All the samples were degassed at 150˚C for more than 6 h prior to the Nitrogen sorption tests. Raman spectra were collected on LabRAM (Horiba Ltd) with 532 nm laser. X-ray diffraction (XRD) patterns were collected on a powder X-ray diffractometer at 40 kV and 15 mA using Co-Kα radiation (Miniflx-600, Rigaku).

D. Electrode Preparation and Electrochemical Measurements

All the electrochemical measurements were performed under identical conditions (the same catalyst mass loading). In a typical electrode preparation, 2.0 mg of synthesized catalyst was ultrasonically dispersed in 0.5 ml 0.5 % Nafion aqueous solutions. 20 µL of catalyst dispersion (4.0 mg mL^{-1}) was then transferred onto the glassy carbon rotating disk electrode (RDE, 0.196 cm^2, Pine Research Instrumentation, USA) via a controlled drop casting approach and dried in ambient environment for 1 h and served as a working electrode. 0.1 M KOH aqueous solution was used as the electrolyte, which was purged with O_2 for at least 30 min to achieve O_2-saturated solution. The reference electrode was an Ag/AgCl in 4M KCl solution and the counter electrode was platinum wire.

Cyclic voltammograms (CVs) and linear sweep voltammograms (LSVs) tests were carried out using a glassy carbon rotating disk electrode. The scan rate of CVs was kept as 100 mV s^{-1} while that was 5 mV s^{-1} for LSVs and RDE tests. The data were recorded using a CHI 760D bipotentiostat (CH Instruments, Inc., USA).

The overall electron transfer numbers per oxygen molecule involved in a typical ORR process can be calculated from the slopes of Koutecky-Levich plots using:

$$1/j_D=1/j_K+1/(B\omega^{1/2}) \quad (1)$$

where potential, j_D is the measured current density on RDE, ω is the electrode rotating speed in rpm, and B is the reciprocal of the slope, which could be determined from the slope of Koutecky-Levich plot using Levich equation:

$$B=0.2nF(\nu)^{-1/6}C_{O2}(D_{O2})^{2/3} \quad (2)$$

where n is the number of electrons transferred per oxygen molecule, F is the Faraday constant, ν is the kinetic viscosity, CO_2 is the bulk concentration of O_2, and DO_2 is the diffusion coefficient of O_2 in 0.1 M KOH. The constant 0.2 is adopted when the rotating speed is expressed in rpm.

The stability tests were performed at a static potential of -0.3V vs. Ag/AgCl at room temperature in the O_2-saturated 0.1M KOH aqueous electrolyte. The methanol tolerance of materials was tested under the same condition before and after adding methanol to electrolyte.

III. Results and Discussions

The porous Fe-NPC nanoparticles were prepared via soft-templating method as shown in Fig. 1. The first synthesis step involved in the formation of micelles from the combination of two surfactants F127 and CTAB. Next, aminophenol and formaldehyde precursors were polymerized on the surface of micelles to form a resol-micelle complex through a sol-gel process at 30˚C followed by introduction of $FeCl_3.6H_2O$ as iron-precursor. Following the cross-linking of Fe-contained resol and the aggregation of nanomicelles under a hydrothermal treatment at 100˚C, the as-synthesized porous polymer nanoparticles were obtained. Afterwards, soft-templates were removed by heating at 350˚C (rate of 1.5˚C/min) for 3 h and Fe-NPC nanoparticles were formed by direct carbonization at 900˚C (rate of 2˚C/min) for 4 h under N_2 flow.

The morphology of Fe-NPC nanoparticles was first investigated by scanning electron microscopy (SEM) and transmission electron microscopy (TEM). The SEM images show that Fe-NPC nanoparticles are approximately spherical in morphology and they are in the same dimensions (Fig. 2 (a)).

TEM images confirm the spherical morphology with average particle diameter of 100 nm and presence of iron species (Fig. 2 (b)). Both SEM and TEM images show that spheres are randomly stacked together which might be attributed to defective structure of synthesized spheres due to presence of doped nitrogen and metal species [17]. Fig. 2 (c) exhibits the energy-dispersive spectrum (EDS) of Fe-NPC nanoparticles which confirms the presence of iron, nitrogen, oxygen and carbon in the structure of synthesized materials.

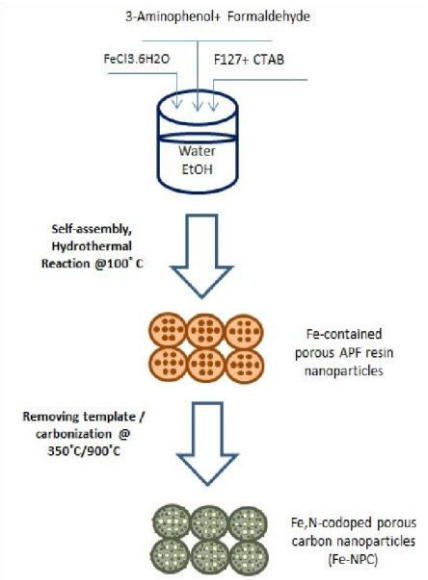

Fig. 1 Synthesis procedure of Fe-NPC nanoparticles

The surface area and porosity of synthesized material was characterized using nitrogen adsorption-desorption technique. The isotherm of the Fe-NPC nanoparticles (Fig. 3 (a)) exhibits the type IV curve with a distinct capillary condensation step at relative pressure (P/P_0) of 0.4-0.6 and a H_1 hysteresis loop, indicative of uniform ordered mesopore structure. The sharp step at P/P_0=0.9-1 corresponds to the capillary condensation of nitrogen inside the extra-large mesopores/macropores which were created by stacking the spheres together [17]. The raised adsorption amount at low presuure (P/P_0<0.05) also suggests the existence of micropores in pore structure of synthesized nanoparticles.

The pore size distribution result shows a sharp peak centered at about 3.8 nm, which confirms the uniform mesopore structure of synthesized materials (Fig. 3 (b)). The BET surface area and pore volume of Fe-NPC nanoparticles were 443.83 m^2/g and 0.52 cm^3/g, respectively.

X-ray diffraction (XRD) was performed to reveal the materials' crystal structure (Fig. 4 (a)). The XRD pattern confirms the existence of Fe species (both metallic Fe and magnetic Fe_3O_4). The XRD pattern also shows a broad XRD diffraction peak at 2θ=24˚ (for both Fe-NPC and NPC materials) which is attributed to the graphitic structure of synthesized nanoparticles and another broad peak at 2θ=44˚ for NPC nanoparticles which confirms the existence of disordered amorphous carbon in its structure [18], [19]. Raman spectra of samples with and without iron content were also collected further assess the graphitic structure of materials. As shown in Fig. 4 (b), Typical G bands representing the sp^2-hybridized graphitic carbon atoms (~1580 cm^{-1}) and D bands resulting from the disordered carbon frames on the defect sites (~1350 cm^{-1}) were obtained [20]. For Fe-NPC nanoparticles, the I_G/I_D ratio increases compared to NPC nanoparticles indicating higher-graphitic structure were formed.

To evaluate the ORR catalytic performance of the synthesized nanoparticles, cyclic voltammetry (CV) was firstly conducted. As shown in Fig. 5 (a), Fe-NPC nanoparticles showed a distinct ORR peak centered at -0.234 V (vs. Ag/AgCl) which is about 192 mV more positive than samples without iron (NPC). Linear sweep voltammetry (LSVs) have been monitored using a rotating disk electrode (RDE) in O_2-saturated electrolyte to further investigate the ORR activity. The onset potential and reaction current density of synthesized materials were acquired from LSVs at 1600 rpm (Fig. 5 (b)). Remarkably, Fe-NPC showed the comparable onset potential with commercial Pt/C (-0.106 and -0.102 V, respectively) and more positive onset potential than NPC nanoparticles (-0.295V). Fe-NMCs also showed highest reaction current density at certain over potential, suggesting the presence of highest number of active site and fastest reaction kinetics of Fe-NPC nanoparticles between other two samples (NPC and Pt/C). A series of LSVs were also recorded from 400 to 2400 rpm for Fe-NPC nanoparticles (Fig. 5 (c)) which show reaction current growth by increasing the rotation speed. Fig. 5 (d) presents the Koutecky-Levich plots of Fe-NPC nanoparticles at different potential obtained from RDE at several rotation rates. Accurate electron transfer numbers (n) and limiting current density (J_k) were calculated through K-L plots and suggesting that oxygen can be reduced on Fe-NPC catalysts in four electron ($4e^-$) reaction pathway with high limiting current density (11.71 $mAcm^{-2}$@ -0.5V vs. Ag/AgCl).

The durability of Fe-NPC nanoparticles was evaluated by the chronoamperometric response under a constant voltage of -0.3V (Fig. 6 (a)) which exhibits a reliable stability, retaining 93% of the initial current after 60000 seconds. The methanol tolerance ability of selected catalyst was tested by monitoring the ORR current after the addition of methanol into the electrolyte solution (with the resulting methanol concentration of 3M). As shown in Fig. 6 (b), there is no significant change on the ORR performance of the catalyst under -0.3V after the addition of methanol into the electrolyte, suggesting the high selectivity of Fe-NPC catalyst towards ORR to avoid crossover effects.

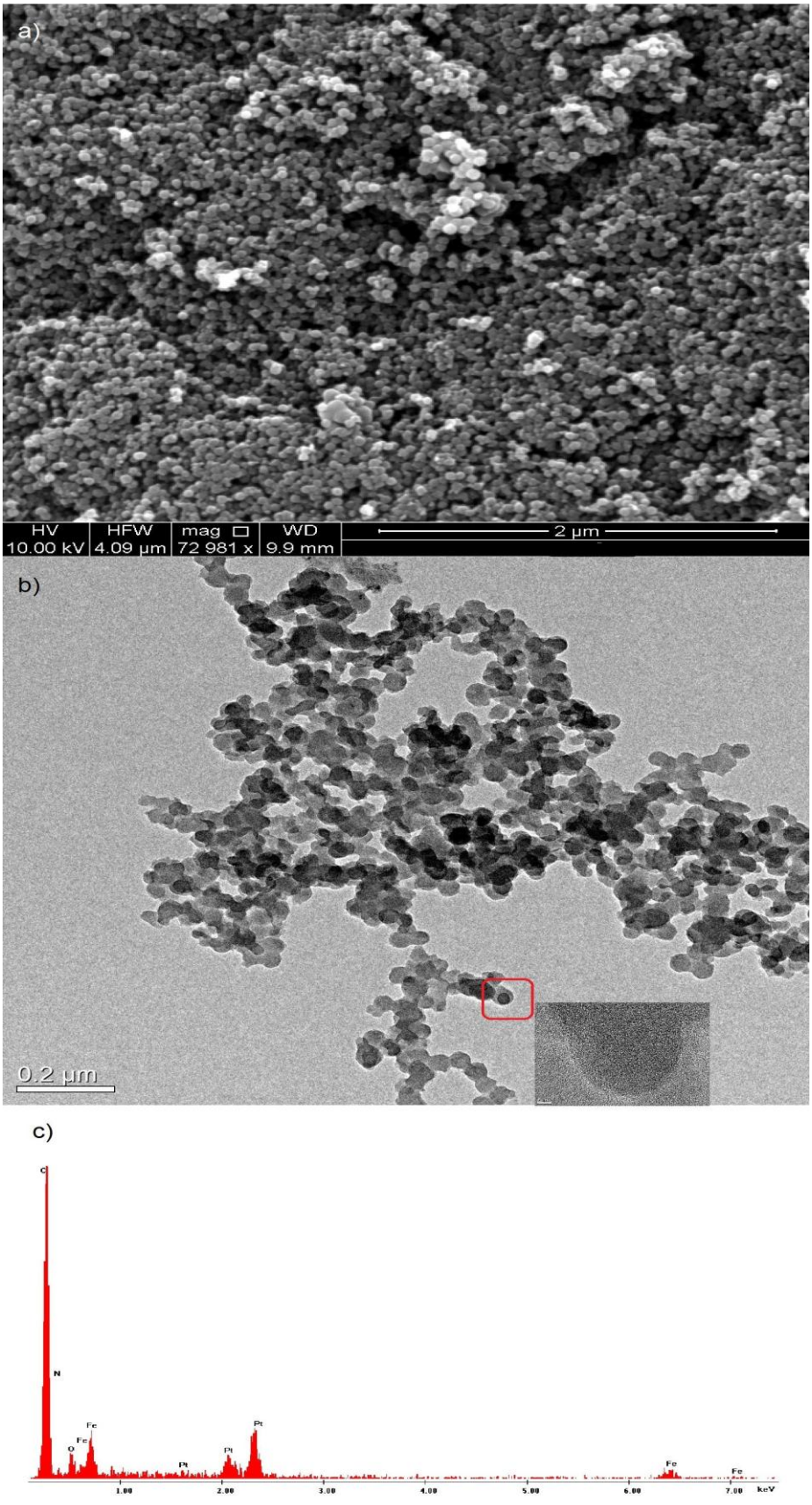

Fig. 2 (a) SEM images, (b) TEM images and (c) EDS spectra of Fe-NPC nanoparticle

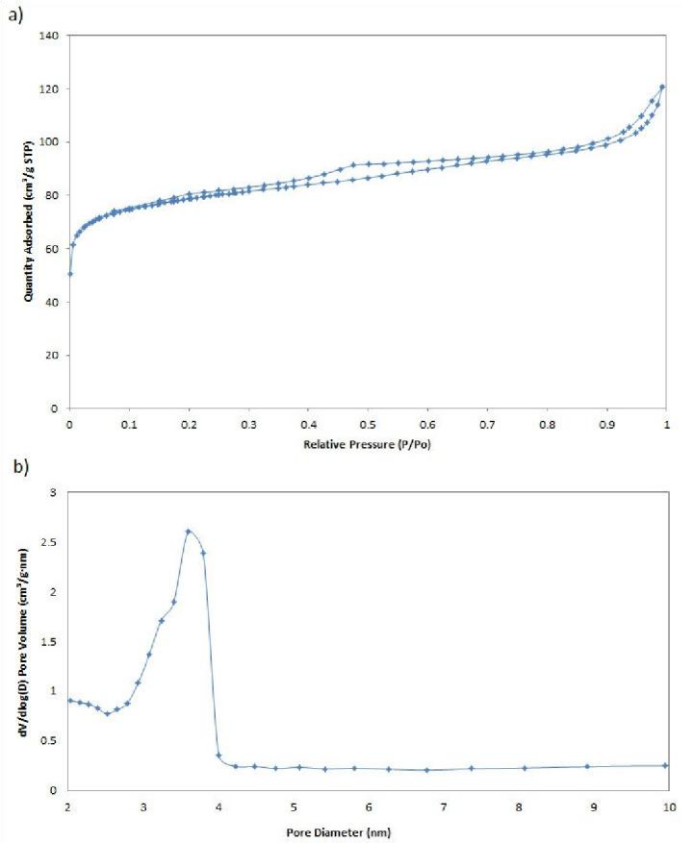

Fig. 3 (a) Nitrogen adsorption-desorption isotherm and (b) pore size distribution of Fe-NPC nanoparticles

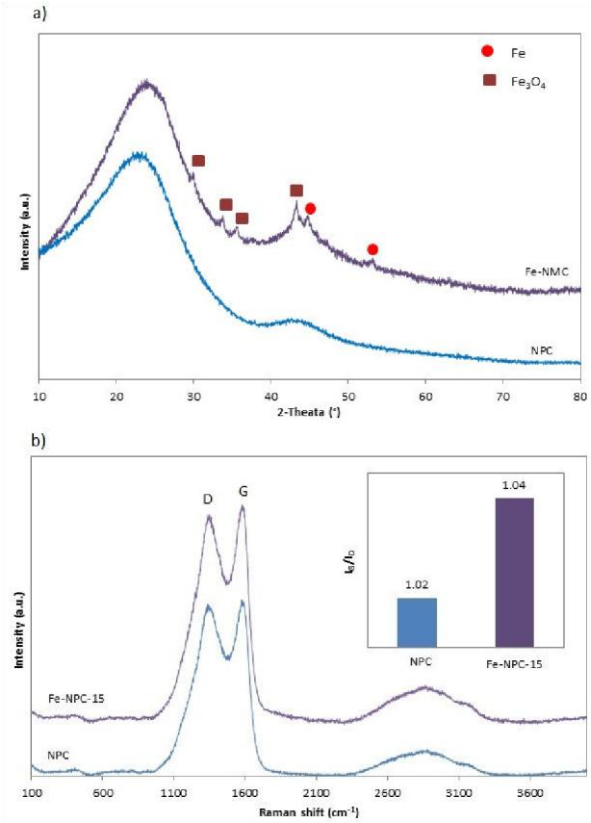

Fig. 4 (a) XRD pattern, (b) Raman spectra and (inset of b) I_G/I_D ratio of synthesized nanoparticles

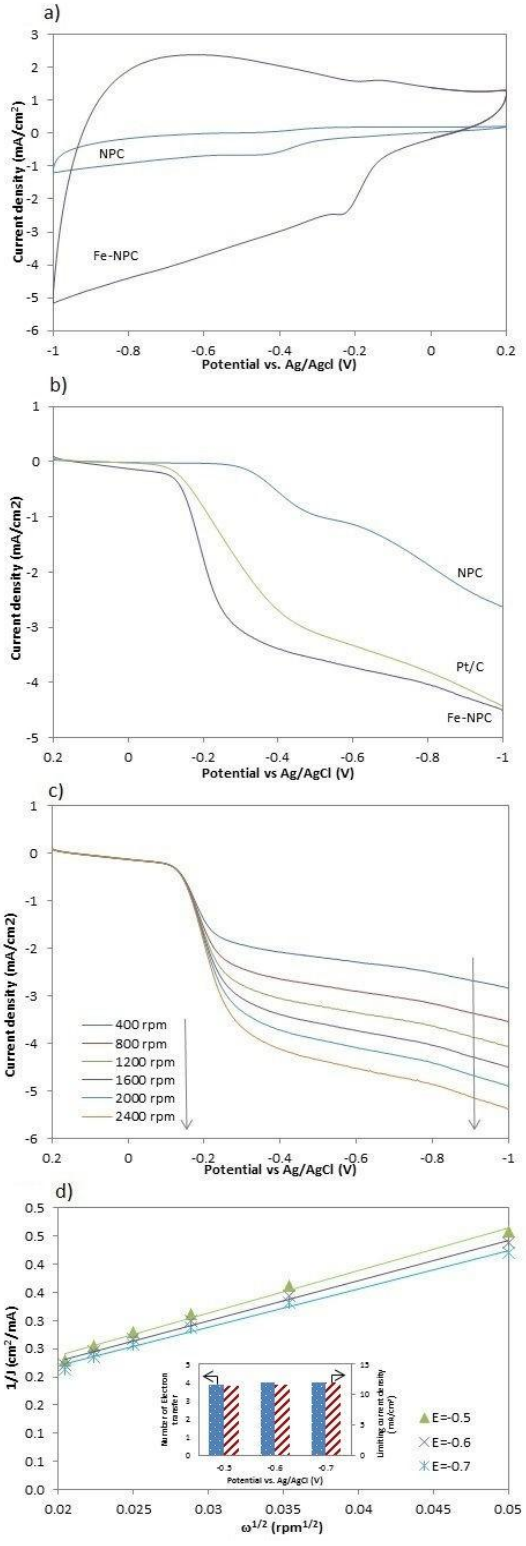

Fig. 5 (a) CVs of ORR on the synthesized electro catalysts in an O2-saturated 0.1 M KOH solution (scan rate: 100 mV s-1). (b) LSVs of synthesized electro catalysts on a RDE (1600 rpm, scan rate: 5 mV s-1), (c) LSVs of Fe-NPC nanoparticles on a RDE (1600 rpm, scan
rate: 5 mV s-1) at different rotating speeds from 400prm to 2400 rpm, (d) K-L plots of Fe-NPC nanoparticles on a RDE

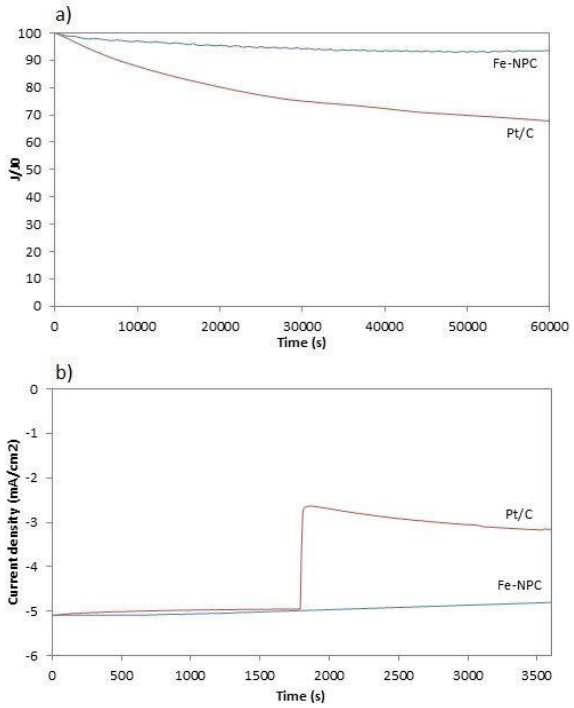

Fig. 6 The chronoamperometric response of Fe-NPC nanoparticles and commercial Pt/C at -0.3 V (a) after 60000 s, (b) after methanol addition

IV. Conclusion

In summary, Fe-NPC nanoparticles has been synthesized via simple and low-cost soft-templating method with good conductivity, mesopore structure, high pore volume and large surface area to catalyze the electron reduction of oxygen. The synthesized electro catalyst exhibit higher ORR activity, more favorable kinetics, stronger stability and durability than those of metal-free NPC and commercial Pt/C. The excellent catalytic performance of Fe-NMC nanoparticles can be attributed to the porous structure, large active surface area, strong structural stability and improved mass/charge transport. This novel approach for fabrication of Fe-NPC nanoparticles could have flexibility in tailoring the composition, mesoporosity, morphology and graphitic structure, which may open a space for the preparation of other metal and nitrogen co-doped carbon materials with even higher performance.

References

[1] Fillol, J.L., et al., Efficient Water Oxidation Catalysts Based on Readily Available Iron Coordination Complexes. Nat Chem, 2011. 3 (10): p. 807-813.
[2] Subbaraman, R., et al., Trends in Activity for the Water Electrolyser Reactions on 3d M (Ni,Co,Fe,Mn) Hydr(oxy)oxide Catalysts. Nat Mater, 2012. 11(6): p. 550-557.
[3] Candelaria, S.L., et al., Nanostructured Carbon for Energy Storage and Conversion. Nano Energy, 2012. 1(2): p. 195-220.
[4] Kunze, J. and U. Stimming, Electrochemical Versus Heat-Engine Energy Technology: A Tribute to Wilhelm Ostwald's Visionary

Statements. Angewandte Chemie International Edition, 2009. 48 (49): p. 9230-9237.
[5] Liang, Y., et al., Strongly Coupled Inorganic/Nanocarbon Hybrid Materials for Advanced Electrocatalysis. Journal of the American Chemical Society, 2013. 135(6): p. 2013-2036.
[6] Steele, B.C.H. and A. Heinzel, Materials for Fuel-Cell Technologies. Nature, 2001. 414(6861): p. 345-352.
[7] Armand, M. and J.M. Tarascon, Building Better Batteries. Nature, 2008. 451(7179): p. 652-657.
[8] Moussallem, I., et al., Chlor-Alkali Electrolysis with Oxygen Depolarized Cathodes: History, Present Status and Future Prospects. Journal of Applied Electrochemistry, 2008. 38(9): p. 1177-1194.
[9] Kinoshita, K., Carbon: Electrochemical and Physicochemical Properties. 1988: Wiley-Interscience.
[10] GreeleyJ, et al., Alloys of Platinum and Early Transition Metals as Oxygen Reduction Electrocatalysts. Nat Chem, 2009. 1(7): p. 552-556.
[11] Mazumder, V., Y. Lee, and S. Sun, Recent Development of Active Nanoparticle Catalysts for Fuel Cell Reactions. Advanced Functional Materials, 2010. 20(8): p. 1224-1231.
[12] Li, X.-H. and M. Antonietti, Polycondensation of Boron- and Nitrogen-Codoped Holey Graphene Monoliths from Molecules: Carbocatalysts for Selective Oxidation. Angewandte Chemie International Edition, 2013. 52(17): p. 4572-4576.
[13] Liang, J., et al., N-Doped Graphene Natively Grown on Hierarchical Ordered Porous Carbon for Enhanced Oxygen Reduction. Advanced Materials, 2013. 25(43): p. 6226-6231.
[14] Zhu, Y., et al., Unravelling the Structure of Electrocatalytically Active Fe–N Complexes in Carbon for Oxygen Reduction Reaction. Angewandte Chemie International Edition, 2014: p. n/a-n/a.
[15] Lv, L.-B., et al., Anchoring Cobalt Nanocrystals through the Plane of Graphene: Highly Integrated Electrocatalyst for Oxygen Reduction Reaction. Chemistry of Materials, 2015. 27(2): p. 544-549.
[16] Wei, J., et al., A Controllable Synthesis of Rich Nitrogen-Doped Ordered Mesoporous Carbon for CO2 Capture and Supercapacitors. Advanced Functional Materials, 2013. 23(18): p. 2322-2328.
[17] Zhang, D., et al., Nitrogen and Sulfur Co-Doped Ordered Mesoporous Carbon with Enhanced Electrochemical Capacitance Performance. Journal of Materials Chemistry A, 2013. 1(26): p. 7584-7591.
[18] Zhao, Y., et al., Nitrogen-Doped Carbon Nanomaterials as Non-Metal Electrocatalysts for Water Oxidation. Nat Commun, 2013. 4.
[19] Sheng, Z.-H., et al., Catalyst-Free Synthesis of Nitrogen-Doped Graphene via Thermal Annealing Graphite Oxide with Melamine and Its Excellent Electrocatalysis. ACS Nano, 2011. 5(6): p. 4350-4358.